Journal of Cleaner Production 186 (2018) 585–601

Contents lists available at ScienceDirect

Journal of Cleaner Production

journal homepage: www.elsevier.com/locate/jclepro

Challenges of digitalizing the circular economy: Assessment of the state-of-the-art of metallurgical carrier metal platform for lead and its associated technology elements

R.F. van Schalkwyk [a], M.A. Reuter [a, *], J. Gutzmer [a], M. Stelter [b]

[a] Helmholtz Center Freiberg for Resource Technology, Chemnitzer Strasse 40, Freiberg, Germany
[b] Institut für Nichteisenmetallurgie & Reinstoffe, TU Bergakademie Freiberg, Leipziger Strasse 34, Freiberg, Germany

ARTICLE INFO

Article history:
Received 3 October 2017
Received in revised form
8 March 2018
Accepted 10 March 2018
Available online 14 March 2018

Keywords:
Circular economy
Lead
Technology elements
Process metallurgy
Resource efficiency
Sustainability

ABSTRACT

The circular economy (CE) paradigm in its broadest sense is key to our survival as a species. Due to this critical importance, understanding its fundamental limitations is thus of significant importance. Especially understanding the losses to Nature are key as these represent the true limitation to circularity. This requires at the minimum an understanding of the thermodynamics and entropy of the losses. Most CE work as well as the many depictions to date neglect to address this in detail, the many losses are brushed aside. Many texts in CE do not use the words entropy, thermodynamics, mass and heat transfer, technology etc. which all ultimately fundamentally affect both the circularity as well as economic viability of the system. Using lead as carrier for the narrative of this paper, the state-of-the art from technology to the thermodynamics as well as heat and mass transfer, product design, modularity, environmental impact, system simulation etc. will be critically discussed. This will reveal what key knowledge and data is presently missing to achieve the economically viable circularity of materials and products. This paper identifies what should be researched and developed to "close" the circular economy system. It thus provides a "ground zero" or baseline for the evaluation of the true economic viability of the CE paradigm relative to what we are presently achieving in our linear economy paradigm.

Contents

* Corresponding author.
E-mail addresses: f.schalkwyk@hzdr.de (R.F. van Schalkwyk), m.reuter@hzdr.de (M.A. Reuter), j.gutzmer@hzdr.de (J. Gutzmer), stelter@inemet.tu-freiberg.de (M. Stelter).

https://doi.org/10.1016/j.jclepro.2018.03.111
0959-6526/

1. Introduction

Ellen Macarthur (2017) defines the Circular Economy (CE) as *"Looking beyond the current "take, make and dispose" extractive industrial model, the circular economy is restorative and regenerative by design. Relying on system-wide innovation, it aims to redefine products and services to design waste out, while minimising negative impacts. Underpinned by a transition to renewable energy sources, the circular model builds economic, natural and social capital."* However, when translating this significant message to images, it is striking that the key extractive industry is not depicted in the Ellen Macarthur depiction and neither in the EU depiction of a CE (EU, 2015).

The Ellen Macarthur definition elegantly describes a CE but negates the losses from each step in the process. Many of these losses are dictated by thermodynamics (which governs the chemical reactions which will take place in a complex system) and complexity due to affinities of materials and metals for each other which downgrades quality and forces refining at the cost of significant entropy creation (entropy is a thermodynamic quantity that makes losses unavoidable). Product design can mitigate some of these losses, but complexity, material functionality and connections render this challenging (Fairphone et al., 2017).

On a strategic level, steps have been identified to guide the economy of metals towards a circular system. This can be seen in publications towards a circular economy such as the EU action plan for circular economy (EU, 2015). However, fundamental aspects are missing in most of the CE documents published thus far. The term entropy is not mentioned in the context of economic feasibility of the CE (Reuter, 2016). Circular economy reviews and special journal editions such as Brocken et al. (2017), with its numerous papers, do not critically discuss the limits of the material processing system in a sufficient fundamentally grounded manner.

To show the key position of the extractive industry in "closing" the loop and highlighting the losses dictated by thermodynamics and product design "mineralogy" (or chemical associations within product parts), the texts of CE have been translated into Fig. 1. Fig. 1 implicitly links energy (the CE is embedded within the renewable energy infrastructure), entropy, mineralogy (products, geological and of residues), product design and extractive industry to the losses from the CE. This fundamental understanding of systems and losses of the CE is discussed by UNEP (2013). While this detail is overlooked in many CE discussions, it is fortunately clearly understood and considered by Fairphone et al. (2017).

A meaningful analysis of the CE can only be made if a detailed understanding is available of the distribution of all metals and materials through the system. Above all, all required thermodynamic data must be available for this analysis. Inherent complexities and associated losses, attributed to associated thermodynamic relationships, have been illustrated by the Metal Wheel (Fig. 2) (Verhoef et al., 2004), expanded for secondary scrap materials as shown in UNEP (2013). This wheel shows succinctly the complexity of a carrier process metallurgical infrastructure.

The metal wheel shows that lead, as well as other base metals such as copper, offer metallurgical platforms to recover many elements in the CE, acting as a source of technology elements from ores and also acting as powerful high temperature liquid metal solvents of minor technology elements during smelting, which are released during refining (Reuter et al., 2015a). Base metals process metallurgy is key to render the CE of many elements feasible, at the lowest nett creation of entropy (Amini et al., 2007). Lead will be highlighted in this paper since copper has recently been highlighted by work such as Shuva et al., 2016b, Klemettinen et al., 2017, Avarmaa et al., 2016 and Avarmaa et al., 2015.

As technology elements play an increasingly important role in today's products, their recovery is paramount and critical requiring detailed understanding. However, there are large and significant knowledge gaps that challenge the optimisation and also the digitalization of the CE to estimate the true losses from it.

Process simulation is crucial to digitalization and optimisation and imparts detailed understanding of all the heat and mass transfer processes within the metallurgical processing technologies (Guthrie, 1993) This makes it possible to quantify the losses from

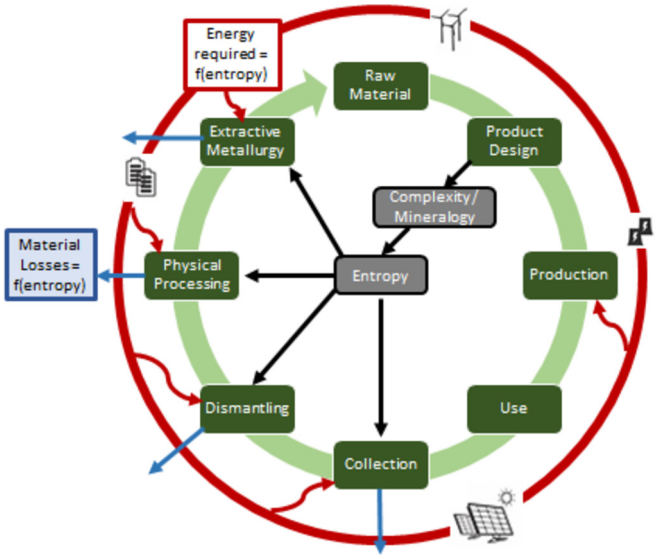

Fig. 1. The CE – Key challenge to harmonize the renewable energy and processing industries through digitalization to optimize resource efficiency.

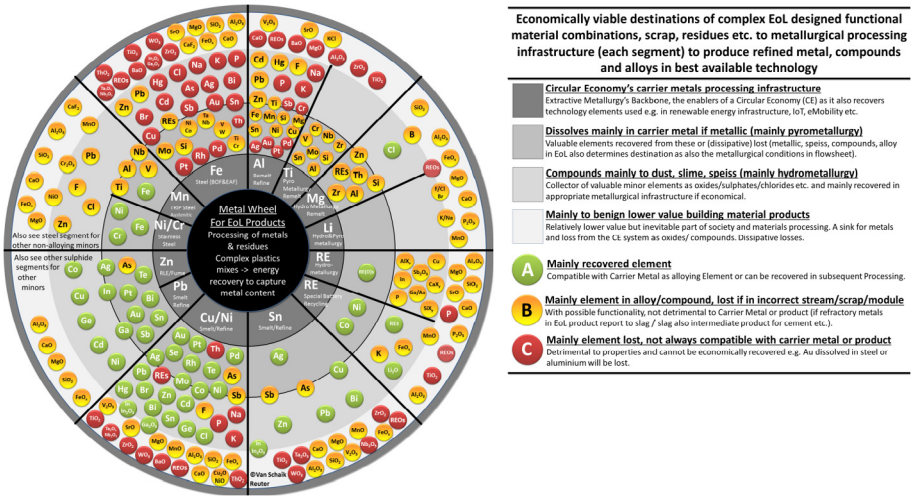

Fig. 2. The metal wheel (Adapted from Verhoef et al. (2004)), showing thermodynamic associations between elements and carrier metals.

the system. Complexity of ores as well as recycled materials and end-of-life (EoL) is challenging the knowledge base and the capability to fully digitalize and quantify the losses from the system using fundamental simulation tools (Reuter et al., 2015b). (Mass transfer within a metallurgical reactor entails the transfer of elements from one phase to another, e.g. from a metal to a slag phase. Heat transfer means the transfer of energy in the form of heat due to a temperature difference.)

To understand the digitalization challenges of the CE, this paper discusses and explores with reference to lead and mineralogical associated zinc and minor elements (a selection of these are sometimes called technology elements) the following aspects:

- **CE and defining process technology and platforms:** The context of process metallurgy within the CE is discussed by providing brief detail on smelters such as Top Submerged Lance-TSL (Errington et al., 2010; Outotec, 2017a), Shuikoushan-SKS (Dongbo, Zunfeng, 2010) and Queneau-Schuhmann-Lurgi-QSL (Siegmund, 2000).
- **Thermodynamic data:** An overview of work that has been done to date on the thermodynamic behaviour of technology elements during pyrometallurgical processing of lead (and associated zinc – Reuter et al., 2015a) is given. It builds on recent overviews and work in copper (Avarmaa et al., 2016; Shuva et al., 2016a, 2016b &2017). Various experimentally determined data are depicted showing the equilibrium distributions of minor elements between slag and lead metal phases at controlled temperatures and oxygen partial pressures. It will become clear that significant work needs to be done to fill the data gaps and define the theoretical process losses.
- **Mass and heat transfer as well as reaction kinetics:** Ultimately, the distribution data must be used in process and reactor simulation models. Therefore, a brief overview of process and reactor simulation will be provided as well as the availability of kinetic models in lead (and the associated zinc) metallurgy.
- **Digitalizing the CE-Process system models and process control:** To evaluate the economics of the CE requires rigorous system simulation approaches (Reuter, 2016).

The above aspects highlight what fundamental information and platforms are lacking to better or even fully describe the CE by rigorous simulation, which is the usual basis for a detailed capital expenditure (CAPEX) and operating expenditure (OPEX) evaluation as well as environmental assessment in the metallurgical processing industry.

This information is critical for the formulation of policy that will enable a smart and versatile metallurgical CE. Frankly, without the metallurgical infrastructure and knowledge available to process materials and complex mixtures, CE will be difficult to achieve.

2. CE and defining process technology and platforms

Lead as carrier metal plays a key role in the CE, both as a provider of technology elements but also as a solvent and thus key link between resource and product. In this section lead production and applications will be discussed, as well as the metallurgical technology that makes lead processing possible.

2.1. CE: lead production, sources and applications

According to the International-Lead-Association (2012), 54% of Pb was sourced from secondary sources worldwide in 2012, which increased to 58% in 2016 (Fig. 3 - International-Lead-and-Zinc-Study-Group, 2017).

Primary lead smelters typically process a mixture of concentrates (e.g. PbS, $CuFeS_2$, ZnS), secondary material, residue material, fly ash and waste slag. Some minor elements occurring with galena are today referred to as technology metals as they feed hightech applications, consumer goods etc. and often also have a positive association with the main mineral element, as can been seen in the Metal Wheel (Verhoef et al., 2004). These minor elements present a metallurgical challenge: they can pose an environmental hazard, decrease the value of the final product or can also be recovered as economically valuable by-product, depending on how the system is managed. Lead in tandem with copper play crucial roles to help "close" the loop of the many elements that appear in End-of-Life (EoL) products and residues.

Lead (and also copper) importantly acts as a collector (solvent phase) for technology elements in the CE, from which they are separated by metallurgical refining processes (Reuter et al., 2015a). The most significant portion of lead use (85%) is for the manufacture of low cost lead-acid batteries. Secondary smelters might need to deal with a variety of materials, including lead metal, battery paste (PbO_2, PbO, $PbSO_4$), used cathode ray tube monitors (Ellis and Mirza, 2010) and materials such as roof flashings, cladding, medical

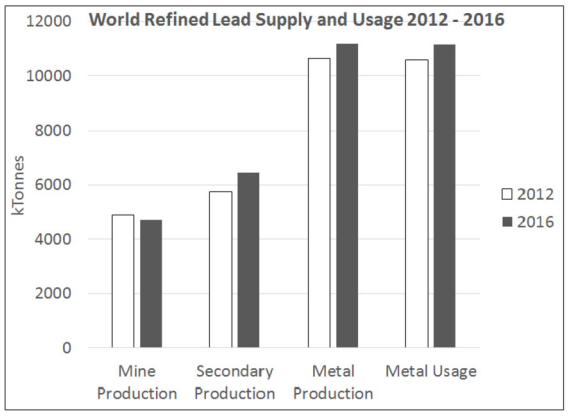

Application	% of Lead Usage
Batteries	85
Cable Sheathing	0.9
Rolled & extruded	3.6
Shot/Ammunition	1.4
Alloys	1.3
Pigments and Compounds	5.5
Miscellaneous	2.2

Fig. 3. Summary of world Lead Production and Usage 2012–2016 (International-Lead-and-Zinc-Study-Group, 2017) (Left). Lead applications according to 2012 statistics (International-Lead-Association) (Right).

equipment (International-Lead-Association, 2012), electronic scrap (soldering) and PCBs; all bringing a multitude of elements to the process (Volodchenko et al., 1983; Shuva et al., 2016b). Due to increased waste recycling, chromium and sodium content in lead smelting slags are increasing (Matsura et al., 2011). Also of importance is the careful management of Ni, Se and Te, since these cause evolutions of H_2 and O_2, which can lead to rapid battery failure (Ellis and Mirza, 2010).

2.2. CE: metallurgical knowledge and technology enablers

The importance of metallurgical knowledge for CE has been highlighted by UNEP (2013) and Fairphone et al. (2017). Primary metal deposits are becoming increasingly more complex and the proportion of complex and unique secondary metals is also increasing (Frenzel et al., 2017a&b). This complexity could be addressed by a design-for-recycle approach, in which the product can be disassembled and grouped into components of similar composition (Van Schaik and Reuter, 2014). However, this approach is not always possible, meaning that metallurgists need to generate knowledge of how these complex metal mixtures behave in metallurgical processing infrastructure (infrastructure = linked processing facilities, flowsheets and reactors).

The metallurgical internet of things, a connection of various processing technology and furnace types linked together by a sophisticated digitalization is shown by Fig. 4. This figure shows the smart linkage of process metallurgy that is required to process complex consumer goods such as Fairphone et al. (2017) to maximize resource efficiency. This can only happen with sufficient understanding of best available technologies (BAT), as mentioned in the next section.

Smart linkage is required at different levels for the circular economy to work. At a high level, linkage refers to steel, aluminium and base metals production facilities which are linked - material is sent to the appropriate facility according to composition. On a flowsheet level, linkage refers to reactors and processes being linked to create an agile system which can be adapted for different feeds. Key to achieving these systems is that digital simulations of the processes must be available, going right down to the reactor models. For the recycling industry, such simulations will make it possible to determine the optimal process routes and also process parameters that can be applied to treat a specific material – this can be done before the material is actually fed into the plant, thus avoiding expensive trial and error. Further, simulations can be run to predict the behaviour of end-of-life consumer goods during recycling. These simulations can inform the design process and

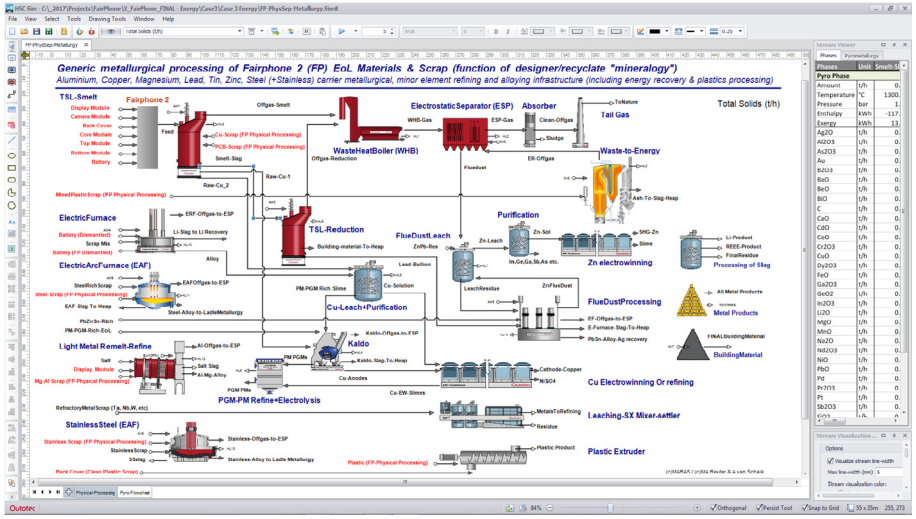

Fig. 4. A system model linking product design to recycling through various metallurgical processing technologies, reactor models calibrated with fundamental data and models as well as experiential information (Fairphone et al., 2017).

consumer goods can be optimised to improve recyclability (minimise energy consumption and maximize recovery during recycling).

The success with which metals in a recycling system can be recovered has often been regarded as dependent on the thermodynamics and transfer processes as well as related economic aspects of the system. An example to apply this knowledge is the 'Metal Wheel', which provides valuable insight for e.g. feasibility studies or determination of legislation. Typically, the distribution of elements between a metal Pb phase and slag phase needs to be understood well. This will be discussed in more detail in Section 3.2.

In practice pyrometallurgical processes are often kinetically controlled. Modelling of actual processes, with the purpose of control and optimisation, requires a combination of thermodynamic and kinetic as well as heat and mass transfer knowledge within the context of the reactor technology. This type of advanced process modelling and control is also important to get metallurgical processes in line with digitalization efforts of society and industry in general (Verhoef et al., 2004). Modelling of pyrometallurgical processes will be discussed in Sections 3.3 and 5.

The metallurgical knowledge and creation of "smart" metallurgical processes and design-for-recycle that are described in this paper should help in optimising operations and therefore bring down the associated cost per tonne of produced metal. Modifications to operations might be required to existing processes to create the flexible flowsheets required for the CE. Government incentives may be required to encourage metal producers to make the CAPEX investment in the CE. Secondly, an economic incentive for the CE can come in the form of informed consumers who purchase products with recyclability and the origin of raw materials as a deciding factor, e.g. consumers who opt for the Fairphone.

2.3. CE: pyrometallurgy as recycling technology platform

Pyro- and hydrometallurgical routes are often employed in tandem to maximize the recovery of metals from resources (Verhoef et al., 2004). Pyrometallurgy is often employed as an initial step for separating elements into slag (which can be cleaned to produce construction material), matte, metal, speiss, flue dust, gas, etc. Hydrometallurgy is used as purification and refining step to create high purity metals (UNEP, 2013). Anindya (2012) discussed the advantages and disadvantages of hydrometallurgy and pyrometallurgy.

The traditional process for primary lead smelting was by means of the sinter-machine (oxidation) followed by the blast furnace or Imperial Smelting (Siegmund, 2000). Direct smelting gained ground since the 1970s (Elvers et al., 1989), due to significant advantages over traditional lead production (Battle and Hager, 1990). According to Sutherland et al. (2013), the following direct smelting furnaces are in operation: Flash smelters such as Kivcet Process, Kaldo or Top Blown Rotary Converter (TBRC), gleaning its development from steelmaking, and bath smelting technologies such as Top Submerged Lance (TSL), Ausmelt/ISASmelt, Shuikoushan (SKS) and Queneau-Schumann-Lurgi (QSL).

It is often wise to optimally link different furnace types to best utilize different transfer phenomena possible in them as Fig. 4 shows for the processing of a mobile phone (Fairphone et al., 2017). Each technology has advantages and disadvantages that can be best exploited in smart flowsheets. An example is control of the oxygen partial pressure. In TSL the oxygen partial pressure is controlled through the slag, in SKS and QSL it is done through blowing through the bullion, for TBRC and Kaldo it is in between as a lance can blow through the slag and impinges on the metal, manipulating the partial oxygen pressure through the lance flame and reductant in the furnace.

The feed composition is an important process variable, which partially dictates the operating slag composition, temperature and partial oxygen pressure (pO_2). Therefore, the feed has to be understood and controlled well for optimal processing. The operating temperatures of lead furnaces can vary greatly, depending on the application, with melting furnaces operating at ~360 °C, blast furnaces at ~1050 °C and smelting at ~1200 °C (Trinks et al., 2004). Operating conditions usually have the slags reaching at least 100 °C higher than the liquidus temperature. The controlling factors for these phenomena are mixing characteristics, transfer processes as well the viscosity of the slag, which is also linked to process chemistry and its governing thermodynamics.

Metallurgical know-how is required to determine how a technology element interacts with the furnace and with the operating conditions.

2.4. CE: what is missing?

This section reflects the available metallurgical "toolbox", but to be optimally effective for the CE, it requires a smart combination and retention of these technologies to maximize resource efficiency - for lead and zinc, but especially also for the recovery of all the valuable technology elements that "fuel" the renewable energy infrastructure that is reflected by Fig. 1. In order for the system to be truly optimised, it needs to be digitalized. The aspects that are required for this to work, which were touched on in the preceeding discussion are:

- systemic understanding and modelling of the systems, flowsheets and process units,
- measured kinetic and thermodynamic data which can be used within unit, flowsheet and system models,
- analyses of big data (operational and laboratory) to calibrate unit models to industrial reality, and
- application of data and unit models within system models with applications e.g. Life-cycle-analyses, CAPEX and OPEX estimations and Design for Recycle.

These aspects have been discussed in extensively by Reuter (2016).

3. Thermodynamic knowledge and data

Considerable fundamental knowledge is required to be able to digitalize the metallurgical infrastructure of the CE and hence to quantify the economic feasibility of Fig. 1. This section will provide an overview of data which is available in terms of thermodynamics. These data can be applied for simulating reactors and flowsheets and also to determine theoretical losses within larger systems. The discussion will consider:

- slags used in direct smelting slag chemistry,
- thermodynamic measurements: (i) methods; (ii) a literature study of thermodynamic measurements that define the behaviour of lead and (iii) thermodynamic measurements for minor elements during smelting,
- complex and volatile metal mixtures (which is not available in literature), and
- FactSage® and HSC as platforms for metallurgical modelling that utilize experimental data (see FactSage (2015) and Outotec (2017b) for more information about these respective software packages).

3.1. Direct Pb smelting slags

In direct lead smelting a large quantity of lead is absorbed during the oxidative stage, which must be rejected during reductive stage (Battle and Hager, 1990). Therefore, slags for direct smelting had to be developed during the 80s. Hollitt (1984a) reported that the basicity of oxides in Pb-Fe-O-SiO_2 slags can be ranked as follows: CaO > MgO > ZnO > PbO > FeO > Al_2O_3 (amphoteric). Therefore, PbO will preferentially bind with SiO_2, when compared to FeO, and unstable FeO becomes prone to form magnetite in the presence of PbO. To counter this, higher silicate content might be required for direct lead silicate slags (Hollitt, 1984a). However, in a high acidic silica slag, viscosity issues might arise.

Yazawa et al. (1981) found that approximately ten times more lead dissolved in iron silicate slags than in calcium ferrite slags. Yazawa et al. (1981), Hollitt (1984a), Rytkönen and Klarin (1987) and Fisher and Bennington (1991) also investigated more basic calcium ferrite slags, due to beneficial properties (high fluidity, low melting point, low volume, less lead dissolution) compared to silicate slags. It was shown by Rytkönen and Klarin (1987) that calcium ferrite slags can be more efficient than silicate slags at removing impurities from lead, although it was suggested that more experiments are needed.

Table 1 shows some of the slag compositions that are in use in industry. As a compromise between calcium ferrite and iron silicate slags, FCS (FeO_x, CaO, SiO_2) are typically used. Schriner et al. (2016) presented a critical review of slag chemistry in lead recycling. Jak and Hayes (2010) described the complex phase thermodynamics of the ZnO-FeO-Fe_2O_3-PbO-CaO-SiO_2 system. More recently Shevchenko and Jak (2017) studied the liquidus of the Pb-Fe-Si-O System in equilibrium with metallic Pb.

To optimize smelting operations, it is important to know the retention of technology elements as a function of partial oxygen pressure, over a range of slag compositions. Thermochemical software such as FactSage® can be used for this type of prediction. While the major components are sorted out, missing is complex mixtures of technology elements and their behaviour as a function of slag chemistry, that arise in the CE.

3.2. Measurement of distribution factors and activities

3.2.1. Experimental methods and data

Distribution factors of elements between lead metal/matte and slag phases are typically measured in a laboratory setup, with different slag compositions, oxygen potentials and temperatures.

Synthetic master alloy and master slag phases are prepared for melting. The master slag might be analysed by Electron Probe Micro-Analysis (EPMA) to determine if the material was completely molten (in which case the sample would be glassy). The slag is milled to a powder and the alloy can be drilled to obtain shavings that can be used in further experiments.

Master slag, master alloy and minor elements are mixed to attain a desired mixture. The mixture is heated in a crucible to the reaction temperature. CO and CO_2 are typically blown through the furnace in a fixed ratio to control pO_2. The crucible is often covered to limit volatilisation of components. After sufficient time for equilibration, the sample is quenched either in inert gas or in water.

Table 1
Slag compositions in direct smelting operations Rytkönen and Klarin (1987).

	(CaO + MgO)/SiO_2	Fe/SiO_2
Kivcet	0.76	1.08
QSL	0.50	0.81
Outotec (during Outokumpu times)	0.78	1.00

Solid slag and metal phases are analysed. Laser-Ablation-Inductively-Coupled-Mass-Spectrometry can be used to determine the bulk chemistry (ICP-MS enables investigation at lower detection limits than ICP-OES). Optical microscopy and Scanning Electron Microscopy (SEM) with Energy Dispersive Spectra Analysis (EDS), as well as X-ray Diffraction, have been used to determine the phase composition and microstructure of the slag (Jak, 2012). The benefit of EPMA is the possibility to determine the composition of the liquid which is in equilibrium with the metal by avoiding crystalized solids in slag (Jak et al., 1995). The drawback of the EPMA is that only selected spots are analysed and therefore the analysis is not fully representative Henao et al. (2010).

EPMA has advanced the experimental investigation of slag chemistry. Quenching of a sample followed by EPMA provides a more accurate analysis than high temperature techniques such as high temperature XRD and solid electrolyte cell EMF measurement. Other applications and benefits of EPMA are listed by Jak et al. (1995):

- the liquidus temperature of the slag melt can be obtained,
- the minimum detection limit for crystalline phases is lower than with XRD or DTA (differential thermal analysis),
- EPMA has been applied to measure spatial differences in composition within the solidified melt, to highlight non-homogenous phenomena that occur within the melt.

Takeda et al. (1980) investigated the ferric/ferrous ratio in the slag by means of volumetric titration.

The distribution-ratio of a metal 'M' can be defined as:

$$L_M^{m/S} = \frac{[pct\ M]}{(pct\ M)} \tag{1}$$

With the parentheses () denoting the concentration by weight of the element in the slag and [] denoting the concentration in the matte or metal phase. For a metal with a valence of 2*v*, the oxidation reaction can be expressed as mono-cation oxide:

$$[M] + \frac{v}{2}O_2 = (MO_v) \tag{2}$$

It has been shown by Takeda et al. (1983) and Yazawa and Takeda (1982) that the logarithm of the distribution factor is linearly proportional to the oxygen partial pressure:

$$logL_M^{M/s} = logC - \frac{v}{2\log(pO_2)} \tag{3}$$

Plotting $logL_M^M$ as a function of pO_2 yields a straight line, of which the slope (-v/2) indicates the oxidation state of the metal (Anindya et al., 2013, 2014).

When the activity coefficient of minor elements in the metal is known, together with the reaction constant K (which is a function of T), it is possible to calculate the activity coefficient of the metal oxide at different temperatures, from the distribution coefficient. The method for this calculation was discussed by Anindya et al. (2013, 2014).

3.2.2. Lead solubility

Lead solubility needs to be understood in conjunction with minor element behaviour as a function of slag composition, temperature and partial oxygen pressure. This is required as an input into the reactor models for control and optimisation of furnaces. Much work has been done to this end, which is summarised below. The experimental conditions used by each author can be foundin the appendix.

PbO content in the slag is proportional to the oxygen partial pressure. PbO acts as a basic oxide and therefore the PbO content in the slag will decrease as CaO content is increased in FCS-type slags. This has been confirmed by Johnson (1983), Taskinen et al. (1984), Fisher and Bennington (1991), Moon et al. (1997) and Kudo et al. (2000).

Taskinen et al. (1984) found that an increase of the CaO or PbO content in the slag lead to an increase in the Fe^{3+} in the slag – therefore increasing the possibility of magnetite formation. Rytkönen and Taskinen (1986) found similar results in terms of Fe^{3+}.

Matyas (1975) investigated FeO-Fe_2O_3-CaO-SiO_2-Al_2O_3 slag in equilibrium with lead and found that the activity coefficient of PbO lowered with increased alumina content and that the dissolved PbO therefore increased. It was found that volatilisation depended on the type of crucible - 20% of Pb loss in the case of alumina crucibles, but less than 5% for zirconia crucibles.

Johnson (1983) investigated lead losses to slag at conditions applicable to blast furnaces. They found that the loss to slag increased with increasing FeO/SiO_2 ratio. However, Taskinen et al. (1984) studied FCS slags and found that Pb loss to slag could be minimised by operating at Fe/SiO_2 over unity.

Kudo et al. (2000) investigated PbO dissolution in FCS slag at iron saturation and temperatures of 1150–1250 °C. Temperature did not have a significant impact on the activity coefficient. The data were used to optimize a slag model in FactSage®. Henao et al. (2010) found good agreement between measured data and predictions from FactSage®.

Matsura et al. (2011) investigated Pb dissolution in iron-saturated FeO_x-CaO-SiO_2-$NaO_{0.5}$ and FeO_x-CaO-SiO_2-$CrO_{1.5}$ slags in comparison to an FCS system. The experimental conditions are given in more detail in the Appendix. The activity coefficient of PbO was determined over a range of Cr and Na concentrations. In an FeOx-SiO_2 slag, addition of Na_2O increased the activity coefficient. In a CaO rich slag, Na_2O decreased the activity coefficient. Addition of Cr_2O_3 lead to increased activity of PbO.

Volodchenko et al. (1983) described the lead distribution between lead-copper alloy and slag by a model of oxide solubility from Timucin (1980). The model inputs were lead activity in the alloy and oxygen partial pressure. Hollitt (1984a&b) created a model, based on the free energy of mixing of PbO in silicate slags, to predict the PbO activity. Schlesinger (1986) equilibrated slags and created an empirical model which they compared to Hollitt (1984a&b) but found discrepancies between the two. The PbO content was proportional to the lead activity and ferric/ferrous ratio (which agrees with Rytkönen and Taskinen (1986)) but decreased with increased CaO/SiO_2 ratio. Battle and Hager (1990) collected data on PbO activities in slag and created a regression model to predict the activity, based on weight % of slag components. CaO was the strongest determinant and SiO_2 was not included in the model.

3.2.3. Thermodynamic equilibrium for minor elements: Literature study

A summary of previous distribution factor studies is given in Appendix 1 (table with list of authors and their experimental conditions) and Appendix 2 (studies sorted according to element), with significant findings from each work, including effects of temperature, slag composition and pO_2. Similar recent work has been done for copper (Shuva et al., 2016a; Klemettinen et al., 2017; Avarmaa et al. 2015, 2016). It should be noted that the figures (a to h) in Appendix 3, which can be used to determine the oxidation state of elements in the slag, were recreated from figures that are available in literature - straight lines (with a marker at each end) were either obtained by directly copying the line from the referenced source, or by fitting a straight line the the raw data from the source. The accuracy of the straight line fit is not indicated here - it is recommended to refer to the original works to confirm the interpretation of the data.

3.3. Interactions in complex mixtures: not in literature

The following are shortcomings with slag-liquid metal equilibrium measurements approach:

- In gas-blown reactors the system is open and therefore not in thermodynamic equilibrium, meaning that kinetics control the process. Yet the kinetics are generally not investigated and the gas phase is not reported on in equilibrium investigations.
- Real feeds to reactors could contain up to 60 elements from which compounds can arise. The formation of compounds affects vapor pressure, e.g. SeTe, SePb and TePb, which are more volatile than Se or Te (if the pO_2 is such that these elements are in elementary form).

3.4. Thermodynamic models using activity coefficients and distribution factors in FactSage® and HSC chemistry 9.0

Experimentally measured data are typically incorporated into platforms such as FactSage® or Outotec HSC Chemistry® to model processes.

FactSage® uses a Gibbs energy minimisation sequence to determine phase equilibria. The program possesses a large database of pure element and solution thermodynamic data, including the FSLead database for behaviour of metals in solution in lead and the FTOxid database which includes slag phases and can be used to model dissolution of minor element oxides in the slag. Non-ideal solution behaviour has been modelled over a wide range of compositions. Messner et al. (2007), as well as Antrekowitsch et al. (2006) did work to model the distributions of minor elements during secondary copper smelting, using FactSage®.

Outotec HSC Chemistry® (Outotec, 2017b) provides a platform for the creation of metallurgical flowsheets, which is supported by a Gibbs energy minimisation tool which makes it possible to determine equilibrium compositions at different operating conditions. A present disadvantage of HSC to FactSage® is that the HSC database does not include non-ideal solution behaviour yet – the input of activity coefficients is a requirement if non-ideal solution behaviour is to be modelled (but the input is possible if activity coefficients have been measured). However, well-calibrated models exist for flash smelting that control industrial furnaces using real-time HSC Sim process models advising operators (Outotec, 2017b). An example of the application of HSC Sim is Swinbourne and Kho (2012) who modelled minor element behaviour in copper flash converting. For this type of modelling, the measured distribution coefficients are inputs.

4. Mass and heat transfer as well as reaction kinetics

As will be shown by Sections 4.1–4.3, significant work needs to be done to measure laboratory kinetic and activity data. These aspects are often neglected and only thermodynamics are considered when modelling pyrometallurgical processes (Guthrie, 1993). It is necessary to merge these data with real-time models using sophisticated big-data analysis techniques in combination with fundamental modelling approaches. This type of work requires knowledge of sampling theory and statistically correct use of operational data (UNEP, 2013). Furthermore, significant work should be done to fully develop reactor models that integrate thermodynamics and kinetics into CFD type models. This will help

to further develop technology as well further maximize resource efficiency of the metallurgical industry and thus also of interconnected systems of the CE.

4.1. Measurement of kinetics and dynamic reactor models

Pomfret and Grieveson (1983) reviewed techniques for high temperature kinetic measurements. Sohn et al. (2004) can also be consulted for methods of measuring high temperature kinetics.

To determine kinetic parameters, experimental data needs to be fitted to a model of rate-determining steps. Due to the high temperature, it can often be assumed that the chemical reactions will be fast, and the process rate will be controlled by transport phenomena:

- Transport phenomena over boundary layers at metal/slag interface.
- Gas-liquid mass transfer.

Fundamental, mechanistic kinetic models in lead metallurgy are scarce. Only one study was found on the reduction kinetics of PbO-SiO_2 slag with solid carbon (Kinaev et al., 2005). The rate of gas evolution was found to be chemical reaction controlled at the gas-solid reaction interface.

Dynamic models have been produced in non-lead metallurgy: Richards et al. (1985) presented a mechanistic model for zinc slag fuming by converting, in three papers. The model was constructed from operational data and included process kinetics. This was followed by a similar model by Cockcroft et al., (1988). Kyllo and Richards (1998) modelled the behaviour of minor elements in copper converting based on kinetics, using data such as activity coefficients, vapor pressures and diffusivities from literature. Asaki et al. (2001) investigated the kinetics of copper sulphide smelting in the Mitsubishi process and modelled the effect that the rates of silica and concentrate dissolution, as well as liquid/gas mass transfer rates have on the process.

Sohn et al. (2004) oxidised matte by bubbling oxygen through a submerged lance. The rate of volatilisation of minor elements was controlled by diffusion through the gas film boundary layer around bubbles in the melt and a mass transfer model was developed. Kawai, Shinozaki and Mori (1982) modelled the transfer rate of manganese across a Fe-slag interface. Perez-Tello et al. (2004) measured kinetics of selenium and tellurium removal in a precious metals refinery using a Kaldo furnace.

Clearly, although models have been developed, there is a lack of kinetic models and data in lead metallurgy.

4.2. CFD (computational fluid dynamics) modelling

CFD modelling creates the possibility of coupling flow aspects in a reactor with the chemical reactions to create dynamic furnace models (Guthrie, 1993). CFD-based work has been done to evaluate zinc slag fuming in a TSL furnace (Huda et al. (2012b)) and tuyere-blown furnaces ((Huda et al., 2012a)). These models can predict aspects such as jet penetration, temperature distributions and fuming kinetics. A lack of kinetic models limits the further development of multi-metal recovery models from complex feeds.

4.3. Neural networks – big data analysis

Measurement of data in real-time within the high temperature and harsh smelting environment of metallurgical furnaces remains a challenge. To estimate distribution data for complex feeds in different reactor types requires the use of sophisticated tools to at least calibrate models in a sufficient manner. This is required to produce process models such as depicted by Fig. 4.

Reuter et al. (1992) trained neural networks to predict the activity coefficients of metals and distributions of metals between slag-metal systems, based on data from literature and industry. Aldrich et al. (1994) showed that it is possible to train neural nets on experimental data to predict distribution ratios as well as the oxidation states of elements in the slag. Georgalli et al. (2002) demonstrated a hybrid modelling approach to incorporate thermochemistry and system dynamics to predict process chemistry in an Ausmelt® converter. A neural net was trained on equilibrium data from FactSage® to predict thermodynamic equilibrium and these results combined with autoregressive components (stochastic, time delay, measured history values) to create a modified autoregressive moving average model (ARMAX) to predict actual chemical compositions.

5. Digitalizing the CE-Process system models and process control

To evaluate the economics of the CE requires rigorous data and system simulation approaches (Reuter, 2016). These are crucial to operational control and optimisation and have been used to compare the environmental impact of different technologies and flowsheets. Furthermore, this digitalization permits the linkage of product design, the bill of materials and full material declaration to metal production, thus permitting the estimation of the true recyclability of products and all its contained materials and thus elements.

5.1. Process simulation and life-cycle analysis (LCA)

Linking engineering simulation e.g. HSC Sim (Outotec, 2017a) to life cycle assessment tools e.g. GaBi (2017), it becomes possible to evaluate the environmental footprint of different reactor types, or of entire flowsheets and comparing from the same baseline (Reuter et al., 2015b). When coupled with element and compound data, this tool makes it possible to evaluate the environmental impact when flowsheets are optimised for the management of the technology elements and carrier metals. These approaches were advanced further to estimate the full footprint of systems (Rönnlund et al., 2016). Linking of engineering simulation with LCA tools also makes it possible (as early on as during the product design stage) to evaluate the environmental impact of recycling a product and therefore to optimize the design.

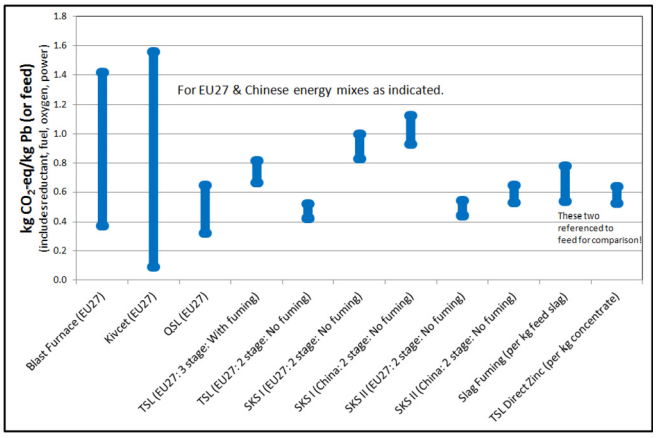

Fig. 5. A comparison of the Global Warming Potential (GWP) $kgCO_2$-eq/kg Pb for different reactor types for lead and zinc production as well as for the recovery of technology elements (Reuter et al., 2015a).

Fig. 5 compares furnaces in terms of Global Warming Potential (GWP). While each type of technology provides benefits, ultimately the carrier metallurgy dictates the footprint, thus its thermodynamics, mass and heat transfer and flow characteristics within the technology. For this reason, the technologies will ultimately all have footprints approximately in the same ballpark. Their capability to deal with minor and technology elements is different. It becomes interesting if all elements are considered simultaneously in complex flowsheets such as shown by Fig. 4. This will ultimately determine the footprint of the CE. This can obviously only be done by rigorous simulation tools as shown or mentioned in this paper.

Verhoef et al. (2004) illustrated by the use of dynamic process simulation the complex dynamic interaction of Ag, Au, Bi, Cu, Fe, Ni, PGMs, Pb, Sn and Zn on each other to show the effect of carrier process metallurgy on the supply and availability of metals for lead containing and lead free solders. The interesting aspect of this work was that it showed the dynamic interactions if one remove lead from solder, while at the same time lead was supplying the elements from the ores that were replacing lead. This work showed and illustrated the intricate non-linear interactions as well as the dynamic effect on the environmental footprint of the CE, for the few elements for which reasonable data exists. CE discussions generally still neglect to include this rigorous detail to fully understand the complexity of the CE.

5.2. What fundamental element data is available or missing to fully assess the CE

Simulation models as shown by Fig. 4 require deep fundamental insight, industrial knowledge and experimental and industrial data measurements for calibration. To this end, this paper reviewed experimentally measured equilibrium distributions as functions of operational conditions (Appendices 1, 2 and 3). The activity coefficients of several metals in the slag have been reported. These data are not necessarily available in environmental databases and this paper should prove a valuable resource which can be applied in system models of the CE.

Furthermore, the following oxidation states have been reported for metals in the slag: Ag^0 or Ag^+ (uncertain), As^o and As_2O_3 (mixture), Bi or BiO (uncertain), Co (inconclusive), Cu_2O and CuO (mixture), GeO, InO or In_2O_3 (uncertain); In_2O is volatile and likely to be in the gas phase in a reactor flowing large volumes of gas through slag, Sb^0 or Sb^{3+} (dependent on pO_2), and SnO, $TlO_{0.5}$, ZnO, PbO. The oxidations states may all affect the elution behaviour and must be considered rather carefully in view of environmental impact.

Of the metals listed as critical by the European Commission Ad Hoc Working Group on Critical Materials (EU, 2017), data was only found for Sb, Bi, Co, Ge and In. Metals listed as critical by the European Commission (EU, 2017), but for which data was not found are Be, Ga, Mg, Nb, Platinum Group Metals, Heavy and light rare earth elements as well as Sc, Si, Ta, W, V. Some elements of importance in lead metallurgy, for which information was not found, are Au, Cu, Ni, Se, Te and Cr.

Experimental measurements on the kinetics of minor element distribution or evaporation is extremely scarce. So are kinetic models of reactors which can be used for CFD modelling. In the absence of these data, the critical questions can be asked:

- How can the CE be fully evaluated for economic and environmental viability?
- How can reviews such as Brocken et al. (2017) provide a serious basis for CE discussions?
- What should the data basis look like to address the complexity of the CE?
- Can we predict true losses in the CE?
- How can we optimize models such as predicted by Fig. 4?

5.3. Linking product and process design to process metallurgy: what simulation platforms are lacking?

This paper has documented various studies that link aspects of Fig. 1 in a fundamental manner. Examples such as the following already exist albeit that in some cases fundamental data had to be estimated from industrial experience not generally accessible to the scientific community:

- In the work for Fairphone et al. (2017), Van Schaik and Reuter (2014) link product design to the process metallurgy of elements, materials, alloys and various plastics for energy and material recovery. It demonstrates the state-of-the-art in digitalizing the CE, from product design to metals recovery on the back of carrier metal processing metallurgy for 46 elements and their functional materials. Greenpeace (2017) has also acknowledged this depth in their evaluation of product design.
- Amini et al. (2007) show the limits of recycling and of achieving CE based on fundamental physics. However, not all thermodynamic data are available to estimate the exergy creation in systems.

The CE community needs urgently to have available missing fundamental thermodynamic and mass and heat transfer data to improve their rigour, thus move beyond Excel-based material flow analysis to be able to understand the systems at hand with rigorous simulation. Such simulation is the usual basis for engineering to produce a detailed feasibility study and thence quantitative CAPEX and OPEX information. System models are required to fully estimate the losses and viability of the CE.

To improve the basis of the CE simulation models, parameterisation must improve as have the process and furnace/technology models. Examples have been given of different furnace models from literature, which include models that assume thermodynamic equilibrium, incorporated a mechanistic understanding of kinetics and flow phenomena or used neural nets which were trained on experimental or operational data. Computational fluid dynamics models must also include more kinetic models of minor and technology elements so that these can be optimally recovered. These models can be employed in process optimisation, but rely on accurate supporting data.

6. The grand challenge of simulating the CE and quantifying the losses in Fig. 1

This paper has reviewed literature on a metallurgical understanding of the behaviour of technology elements in lead metallurgy, which is a key to the CE. The paper further reviewed various simulation and modelling techniques available to critically evaluate the CE to understand its true economic losses.

In summary, this paper shows that the following need to be addressed, developed and measured to fully realize the potential of the CE:

- **Measuring thermochemical data (as presented in Appendices 1,2 and 3):** There are large gaps both in thermodynamic and kinetic data describing the distribution of elements between lead bullion, slag, speiss, gas phase, flue dust etc., that require to be measured or estimated and made available to the scientific community to improve the resource efficiency estimates of the

CE. Presently these can only be estimated if deep understanding of the systems is present by people experienced in the art.

- **Simulating mass and heat transfer processes:** These data can then find their way into more sophisticated modelling platforms such a CFD that can then be used to optimize flow in the systems and hence maximize resource efficiency. There is still considerable work to be done in this arena.
- **Artificial intelligence linked to process models:** Big data analysis combined with rigorous process models can help further to estimate distribution data from real-time measurements and augment laboratory measurements. This builds on work done in the 80s and 90s.
- **CE System simulation:** To systemically optimize the CE system depicted by Fig. 1 requires the detail of the previous points. While rather sophisticated system models already exist, their predictive capability can further be improved if the above fundamental detail improves, especially the deportation and dissipation of critical elements can be understood better.
- **Simulation based Design for Recycling and foot-printing:** While models exist that link product design and the bill of materials to extractive process metallurgy and environmental models, ultimately computer aided design should provide design detail in a form that has thermochemical meaning so that true simulation of the system can be performed. This thermochemical basis linked to element distribution thermodynamics will provide detail on exergetic flows as well estimating and understanding the true entropy limits of the CE.
- **Environmental labelling:** Labelling has advanced recently. Underpinning these with more and improved fundamentally measured distribution data can help to further inform product design as well as the consumer (Greenpeace, 2017; Fairphone et al., 2017).
- **Policy:** Often missing in present CE policy discussions is the realization that a smart and agile metallurgical infrastructure must be present (as reflected by Fig. 2) to make the CE work. Without the metallurgical infrastructure available to process materials and complex mixtures, CE will be difficult to achieve.

If the above is in place, understanding all losses from the system, the grand challenge of simulating the CE is within reach, its true CAPEX and OPEX quantified and its economic viability revealed. This paper, therefore, suggests that much more rigour must flow into the CE discussion to ensure that its true potential is realized. In other words, we must base future discussions on the above-mentioned rigour and advance the less rigorous depictions of CE to this level.

Appendix 1. Summary of the distribution measurement studies between lead and different slag types and temperatures suitable for different furnace technologies

Element Investigated	Comment	Temp. Range	log (pO_2)	Slag Chemistry	Reference
Cu, Ag, Bi, As, Sb, Pb	Also investigated the activity coefficient of PbO in the slag	1200 °C&1300 °C	−13 to −8	58%FeO-3%Fe_2O_3-16%CaO-21%SiO_2-Al_2O_3 or 58%FeO-5%Fe_2O_3-21%CaO-16%SiO_2-Al_2O_3 In iron crucibles	Matyas (1975)
Cu, As, Sb, Bi, Ag, Pb	Investigated equilibrium between Pb-Cu alloy and slag to choose the best operating conditions for direct smelting	1250 °C	−6 to −3	5% or 20% Cu in alloy 40% Fe, 25% SiO_2; 8% Al_2O_3	Volodchenko et al. (1983)
Cu, In, Tl, Sb, Pb	Studied effect of blast furnace slag composition on distribution and the interaction between elements	1200 °C	−12	Approx.: 30% SiO_2; 60% FeO; 8% Fe_2O_3 ~1.3–1.7 FeO:SiO_2 ~0.5–0.75 (MgO + CaO)/SiO_2 Alumina Crucibles	Johnson (1983)
Pb	Solubilities of PbO as applicable to direct lead smelting	1250-1350 °C	−6, −6.5 & −7	FeO_x-SiO_2-CaO $FeO/SiO_2 = 1.660, 0.9295, 0.7773$ $CaO/SiO_2 = 0.4667, 0.6667, 0.8182$ Lime-stabilised zirconia crucible	Taskinen et al. (1984)
Cu, As, Sb, Bi, Zn, Ag, Sn, Pb	Conditions applicable to primary and secondary lead smelting	1200 °C	−7 to −9 SO_2 atmosphere-Pb/PbO ratio used to control oxygen partial pressure	$FeO/SiO_2 = 1.289$ $CaO/SiO_2 = 0.778$	Rytkönen and Taskinen (1986)
Cu, As, Sb, Bi, Zn, Ag Pb	Conditions applicable to primary and secondary lead smelting	1200 °C	−7 to −9 SO_2 atmosphere. Pb/PbO ratio used to control oxygen partial pressure	Calcium Ferrite Slag 25% CaO Rest: Fe + Fe_2O_3	Rytkönen and Klarin (1987)
Cu, As, Sb, Ag, Tl, Bi, Sn	Elements relevant to secondary lead smelting	1150-1300 °C	−5 to −11	FeO_x-CaO-SiO_2 CaO/SiO_2: 0.5–0.8 Fe/SiO_2: 0.8–1.2	Toubarts (1991)
Ag, Cd, Zn, Co, Pb	Possibility of replacing iron silicate slag with calcium ferrite slag	1250 °C	−10	CaO-FeO-SiO_2 MgO crucibles CaO ~16–32% SiO_2 ~ 1–5%	Fisher and Bennington (1991)
Pb, Sb, As, Cu, Ag	Analysis by EMF method as applicable to QSL smelting	1250 °C	−8	PbO-FeO_x-CaO-SiO_2 $CaO/(CaO + SiO_2) = 0.3$ $FeOx/(FeO_x + CaO + SiO_2) = 0.4$	Moon et al. (1997)
Pb		1150-1250 °C			Kudo et al. (2000)

(*continued*)

Element Investigated	Comment	Temp. Range	log (pO_2)	Slag Chemistry	Reference
	Generated large amount of data for slag model in FactSage®		~ −11 to −12 Experiments carried out under argon, slag composition determined oxygen partial pressure.	FeO_x-CaO-SiO_2 Range between iron silicate slags and calcium ferrite slags Iron crucibles	
In	Conditions applicable to primary lead smelting	1200 °C	−10 to −12	FeO-CaO-SiO_2-8% Al_2O_3 Approx. 40% FeO, 30% SiO_2, 20% CaO	Hoang and Swinbourne (2007)
Element Investigated	Comment	Temp. Range	Log (pO_2)	Slag Chemistry	Reference
In, Ge, Pb	Conditions applicable to primary lead smelting	1150–1300 °C	−8 to −12	PbO-FeO-Fe_2O_3-SiO_2-CaO-MgO SiO_2/CaO = 1.6–1.9 SiO_2/Fe = 1	Henao et al. (2010)
Pb solubility	Cr and Na content in secondary/residues was the motivation for the investigation.	1300 °C	−10.75 to −12. Experiments carried out under argon. Fe^{2+}/Fe^{3+} ratio used to control oxygen partial pressure.	FeO_x-CaO-SiO_2-5%$NaO_{0.5}$ FeO_x-CaO-SiO_2-5%$CrO_{1.5}$ Iron crucibles	Matsura, Ueda, Yamaguchi (2011)
Ge	Thermodynamic data generated for process modelling.	1150–1250 °C	−10 to −12.5	9·8 wt-% SiO2, 18·1 wt-% CaO, 49·5 wt-% FeO and 9·7 wt-% Al_2O_3	Yan and Swinbourne (2013)

Appendix 2. Equilibrium studies grouped by elements

Silver (Ag)

Author	Slag System	Temperature Range	Oxygen Partial Pressure	Dissolution State	Activity Coefficient	Comment
Matyas (1975)	FeO-Fe_2O_3-CaO-SiO_2-Al_2O_3	1200–1300 °C	10^{-8} to 10^{-13} atm	Ag^o		
Volodchenko et al. (1983)	High calcium ferro-silicate	1250 °C	$1 \times 10^{-2.6}$ to $1 \times 10^{-5.52.6}$ atm	Ag^o		$L_M^{m/S} = 10^{1.5}$ *to* $10^{2.5}$
Rytkönen and Taskinen (1986)	FeO/SiO_2 = 1.289 CaO/SiO_2 = 0.778	1200 °C	Ar and SO_2 atmospheres pO_2: 10^{-7} to 10^{-9} atm	Ag^o		$L_M^{m/S} = 10^{2.5}$
Rytkönen and Klarin (1987)	Calcium Ferrite 25% CaO 75% Fe and Fe_2O_3	1200 °C	Approx: 10^{-7} to $10^{-8.5}$ atm			Ag reported more readily to the slag than in the case of Rytkönen and Taskinen (1986). Ag reported almost 100% to the metal phase.
Toubarts (1991)	FeO_x-CaO-SiO_2 (CaO/SiO_2: 0.5–0.8, Fe/SiO_2: 0.8–1.2)	1150 and 1300 °C	10^{-5} to 10^{-11} atm			Ag preferentially report to metal, with little dependence on temperature.
Fisher and Bennington (1991)	Compared iron silicate slag with calcium ferrite slag	1250 °C	10^{-10} atm			Nearly all silver reported to metal phase.
Moon et al. (1997)	PbO-FeOx-(CaO-SiO_2-MgO) %CaO/(%CaO+%SiO_2) = 0.4 N_{FeOx}/($N_{FeOx} + N_{CaO} + N_{SiO2}$) = 0.3 to 0.4	1150 °C	$10^{-7.5}$ to $10^{-11.5}$ atm	$AgO_{0.5}$	$\gamma AgO_{0.5} = 4$	$L_M^{m/S} = 2x10^{-3}$ @ $pO_2 = 10^{-8}$ at,

Cobalt (Co)

Author	Slag System	Temperature Range	Oxygen Partial Pressure	Dissolution State	Activity Coefficient	Comment
Fisher and Bennington (1991)	Compared iron silicate slag with calcium ferrite slag	1250 °C	10^{-10} atm			Increase in distribution factor with increased (SiO_2 + MgO) content. Increase in distribution factor with increased CaO content. Significant Co loss due to evaporation.

Arsenic (As)

Author	Slag System	Temperature Range	Oxygen Partial Pressure	Dissolution State	Activity Coefficient	Comment
Matyas (1975)	FeO-Fe_2O_3-CaO-SiO_2-Al_2O_3	1200 −1300 °C	10^{-8} to 10^{-13} atm	Mixture of As^0 and As^{3+}		
Rytkönen and Taskinen (1986)	FeO/SiO_2 = 1.289 CaO/SiO_2 = 0.778	1200 °C	Ar and SO_2 atmospheres pO_2: 10^{-7} to 10^{-11} atm	As^{3+}		Presence of sulphur helped minor elements pass into the slag.
Rytkönen and	Calcium Ferrite 25% CaO 75% Fe and Fe_2O_3	1200 °C	Approx: 10^{-7} to $10^{-8.5}$ atm			

(*continued on next page*)

(*continued*)

Arsenic (As)

Author	Slag System	Temperature Range	Oxygen Partial Pressure	Dissolution State	Activity Coefficient	Comment
Klarin (1987)						
Toubarts (1991)	FeO_x-CaO-SiO_2 (CaO/SiO_2: 0.5–0.8, Fe/SiO_2: 0.8–1.2)	1150 and 1300 °C	10^{-5} to 10^{-11} atm	As^0 and As^{3+} mixture at low pO_2; change to As^{3+} at $10^{-7.5}$ atm		Distribution factor increased with an increase in temperature.
Moon et al. (1997)	PbO-FeOx-(CaO-SiO_2-MgO) $\%CaO/(\%CaO+\%SiO_2) = 0.4$ $N_{FeOx}/(N_{FeOx} + N_{CaO} + N_{SiO2}) = 0.3$ to 0.4	1150 °C	$10^{-7.5}$ to $10^{-11.5}$ atm	As^{3+}	$\gamma AsO_{1.5} = 0.3$ @ 1150 °C	

Copper (Cu)

Author	Slag System	Temperature Range	Oxygen Partial Pressure	Dissolution State	Activity Coefficient	Comment
Matyas (1975)	FeO-Fe_2O_3-CaO-SiO_2-Al_2O_3	1200–1300 °C	10^{-8} to 10^{-13} atm	Mixture of CuO and Cu_2O		Clear difference between alumina crucible and zirconia crucible.
Moon et al. (1997)	PbO-FeOx-(CaO-SiO_2-MgO) $\%CaO/(\%CaO+\%SiO_2) = 0.4$ $N_{FeOx}/(N_{FeOx} + N_{CaO} + N_{SiO2}) = 0.3$ to 0.4	1150 °C	$10^{-7.5}$ to $10^{-11.5}$ atm		$\gamma AsO_{1.5} = 15$ @ 1150 °C	

Bismuth (Bi)

Author	Slag System	Temperature Range	Oxygen Partial Pressure	Dissolution State	Activity Coefficient	Comment
Matyas (1975)	FeO-Fe_2O_3-CaO-SiO_2-Al_2O_3	1200 –1300 °C	10^{-13} to 10^{-8} atm			
Volodchenko et al. (1983)	High calcium ferro-silicate	1250 °C	$1 \times 10^{-5.5}$ to $1 \times 10^{-2.6}$ atm		γBi *in slag* = 0.76	Aluminum vs zirconium crucibles did not have any effect.
Rytkönen and Taskinen (1986)	$FeO/SiO_2 = 1.289$ $CaO/SiO_2 = 0.778$	1200 °C	Ar and SO_2 atmospheres pO2: 10^{-7} to 10^{-9} atm			
Rytkönen and Klarin (1987)	Calcium Ferrite 25% CaO 75% Fe and Fe_2O_3	1200 °C	Approx: 10^{-7} to $10^{-8.5}$ atm			
Toubarts (1991)	FeO_x-CaO-SiO_2 (CaO/SiO_2: 0.5–0.8, Fe/SiO_2: 0.8–1.2)	1150 and 1300 °C	10^{-5} to 10^{-11} atm	Bi^{2+}		Considering Figure d in Appendix 3, there is a range from 0, +2 and + 3 possible.

Tin(Sn)

Author	Slag System	Temperature Range	Oxygen Partial Pressure	Dissolution State	Activity Coefficient	Comment
Rytkönen and Taskinen (1986)	$FeO/SiO_2 = 1.289$ $CaO/SiO_2 = 0.778$	1200 °C	Ar and SO_2 atmospheres pO_2: 10^{-7} to 10^{-9} atm pO_2 was determined from a_{PbO}, which was (measured with electrochemical cell)	SnO		
Toubarts (1991)	FeO_x-CaO-SiO_2 (CaO/SiO_2: 0.5–0.8, Fe/SiO_2: 0.8–1.2)	1150 to 1300 °C	10^{-5} to 10^{-11} atm	SnO		Distribution factor increased proportional to temperature.

Germanium (Ge)

Author	Slag System	Temperature Range	Oxygen Partial	Dissolution State	Activity Coefficient	Comment
Yan and Swinbourne (2003)	CaO (18.1 wt%)–SiO_2 (9.8 wt%) –FeO (49.5 wt%)-Al_2O_3(9.7 wt%)	1150 - 1300 °C	10^{-10} to $10^{-12.5}$ atm	GeO	γGeO = 1.44 to 2.55	13-21% of Ge evaporated; 78–86% found in the slag. SiO_2/CaO and SiO_2/Fe ratios did not affect the evaporation. Temperature changes did not affect distribution coefficient.
Henao et al. (2010)	(PbO-FeO-Fe_2O_3-SiO_2-CaO-MgO); $SiO_2/CaO = 1.6–1.9$, $SiO_2/Fe = 1$	1150 - 1300 °C	10^{-8} to 10^{-12} atm	Reported Ge^{4+}, but graph indicates Ge^{2+} oxidation state		Some Ge evaporated, especially above 1250 °C. No effect from addition of minor elements (Cu, As or Au <5 wt%). Temperature changes did not affect distribution coefficient. Increasing SiO_2/CaO or SiO_2/Fe ratio caused an increase in the distribution ratio.

Thallium (Tl) Although generally present in small concentrations in lead, thallium is a metal of concern due to its' toxicity (Toubarts, 1991)

Author	Slag System	Temperature Range	Oxygen Partial Pressure	Dissolution State	Activity Coefficient	Comment
Johnson (1983)	Fayalite (30% SiO_2, 60% FeO and 8% Fe_2O_3) Fe:SiO_2 ratios of 1.3, 1.5 and 1.7 [(MgO+ CaO)/SiO_2 = 0.5, 0.6 and 0.75)]	1200 °C	10^{-12} atm			Distribution factor: - Increased with (CaO + MgO)/SiO_2 ratio, - Independent of FeO/SiO_2 - Inter-element interactions between In, Tl and Sb (in quantities <1%) was visible at higher basicity ratios.
Toubarts (1991)	FeO_x-CaO-SiO_2 (CaO/SiO_2: 0.5–0.8, Fe/SiO_2: 0.8–1.2)	1150 to 1300 °C	10^{-5} to 10^{-11} atm	$TlO_{0.5}$		Temperature did not significantly influence distribution factor

Indium (In)

Author	Slag System	Temperature Range	Oxygen Partial Pressure	Dissolution State	Activity Coefficient	Comment
Johnson (1983)	Fayalite (30% SiO_2, 60% FeO and 8% Fe_2O_3) Fe:SiO_2 ratios of 1.3, 1.5 and 1.7 [(MgO+ CaO)/SiO_2 = 0.5, 0.6 and 0.75)]	1200 °C	10^{-12} atm			Distribution factor - increased with increased basicity. - Is independent from FeO/SiO_2 - Increased when impurities (0.5–1% of Cu, Tl or Sb) were added to the charge
Hoang and Swinbourne (2007)	40 wt%FeO-20 wt% CaO-30 wt%SiO_2-8%Al_2O_3	1200 °C	10^{-10}, 10^{-11} and 10^{-12} atm	InO	4×10^{-8} to 3×10^{-7}	Distribution factor - Increased with FeO/SiO_2 - Was independent of CaO/SiO_2
Henao et al. (2010)	PbO-FeO-Fe_2O_3-SiO_2-CaO-MgO SiO_2/CaO (wt%/wt%) ratio: 1.1 to 2.1; SiO_2/Fe (wt%/wt%) ratio 0.9 to 1.7	1150 - 1300 °C	10^{-12} to 10^{-8} atm	In_2O_3		Effects of CaO/SiO_2 and SiO_2/Fe changes were uncertain within experimental error. Increasing the temperature increased the distribution factor.

Zinc (Zn)

Author	Slag System	Temperature Range	Oxygen Partial Pressure	Dissolution State	Activity Coefficient	Comment
Fisher and Bennington (1991)	Compared iron silicate slag with calcium ferrite slag	1250 °C	10^{-10} atm			30-70% of Zn lost to gas phase Less than 2% report to bullion Distribution independent of % CaO or %(SiO_2+MgO)
Rytkönen and Taskinen (1986)	FeO/SiO_2 = 1.289 CaO/SiO_2 = 0.778	1200 °C	Ar and SO_2 atmospheres pO_2: 10^{-7} to 10^{-9} atm pO_2 was determined from a_{PbO}, which was (measured with electrochemical cell)			
Rytkönen and Klarin (1987)	Calcium Ferrite 25% CaO 75% Fe and Fe_2O_3	1200 °C	Approx: 10^{-7} to $10^{-8.5}$ atm	ZnO		

Antimony (Sb)

Author	Slag System	Temperature Range	Oxygen partial pressure	Dissolution State	Activity Coefficient	Comment
Volodchenko et al. (1983)	High calcium ferro-silicate	1250 °C	$1 \times 10^{-5.5}$ to $1 \times 10^{-2.6}$ atm	log(pO_2)> −4: Sb^{3+} stable; log(pO_2)< −4: Sb^0 stable		
Johnson (1983)	Fayalite (30% SiO_2, 60% FeO and 8% Fe_2O_3) Fe:SiO_2 ratios of 1.3, 1.5 and 1.7 [(MgO+ CaO)/SiO_2 = 0.5, 0.6 and 0.75)]	1200 °C	10^{-12} atm			Distribution factor: - Independent of (CaO + MgO)/SiO_2 ratio. - Declined sharply with an increase in FeO/SiO_2.
Rytkönen and Taskinen (1986)	FeO/SiO_2 = 1.289 CaO/SiO_2 = 0.778	1200 °C	Ar and SO_2 atmospheres pO_2: 10^{-7} to 10^{-9} atm	Sb^0, but converts to Sb^{3+} above $pO_2 = 10^{-9}$ atm.		
Rytkönen and Klarin (1987)	Calcium Ferrite 25% CaO 75% Fe and Fe_2O_3	1200 °C	Approx: 10^{-7} to $10^{-8.5}$ atm			Lower distribution ratio measured with more basic slag, than in the work of Rytkönen and Taskinen (1986)
Toubarts (1991)	FeO_x-CaO-SiO_2 (CaO/SiO_2: 0.5–0.8, Fe/SiO_2: 0.8–1.2)	1150 and 1300 °C	10^{-5} to 10^{-11} atm			Distribution factor increased proportional to temperature.
Moon et al. (1997)	PbO-FeOx-(CaO-SiO_2-MgO) %CaO/(%CaO+%SiO_2) = 0.4	1150 °C	$10^{-7.5}$ to $10^{-11.5}$ atm	Sb_2O_3	$\gamma SbO_{1.5}$ = 2	Distributes predominantly to metal below log(pO_2) = -8 and to slag above.

(continued on next page)

(*continued*)

Antimony (Sb)						
Author	Slag System	Temperature Range	Oxygen partial pressure	Dissolution State	Activity Coefficient	Comment
	$N_{FeOx}/(N_{FeOx} + N_{CaO} + N_{SiO2}) = 0.3$ to 0.4					

In summary, the distribution factors measured by different authors are in the range of 63–4000. The authors agree that under the studied conditions, silver preferentially reports to the metal. However, some differences should be clarified on whether silver is present in the slag as Ag^o or Ag^+.
It has been observed that As evaporates in the form As_4O_6 (Kawahara et al. (1979).
Information on equilibrium measurements for Bismuth in Lead was found published in five works: Matyas (1975), Volodchenko et al. (1983), Rytkönen and Taskinen (1986), Rytkönen and Klarin (1987) and Toubarts (1991). These works looked at the same temperature range ~1200 °C and within the same pO_2 range ($pO_2 = 10^{-11}$ to 10^{-5} atm), but different slag systems. Significant differences exist between studies for the distribution coefficient values.
From these studies, it appears that Sb can be present as Sb^{3+} or Sb^0 in the slag, although some authors found Sb^{3+} over the entire pO_2 range. There appears to be contradictions in the literature concerning the reaction of Sb to changes in FCS slag basicity.

Appendix 3. Graphs of distribution factors vs. pO_2 (Consult original works for more detailed graphs that include all experimental points)

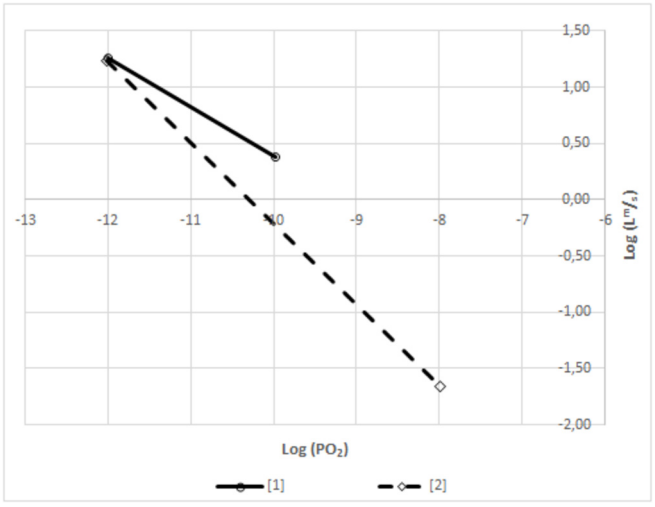

Fig. a. Distribution coefficients for indium, reproduced from Henao et al. (2010), with data from [1] Hoang and Swinbourne (2007) and [2] Henao et al. (2010) at 1200 °C.

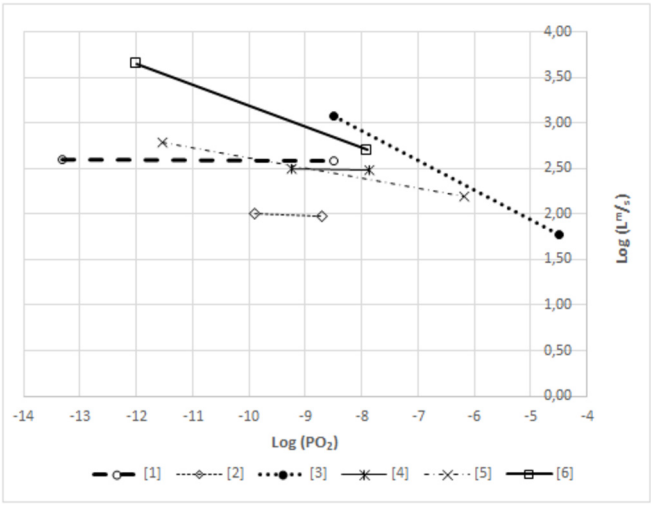

Fig. c. Reproduced from Toubarts (1991). Distribution coefficients for silver at 1200 °C. Data from: [1] Matyas (1975), [2] Volodchenko et al. (1983), [3] Hollitt (1984b), [4] Rytkönen and Taskinen (1986), [5] Toubarts (1991), [6] Moon et al. (1997).

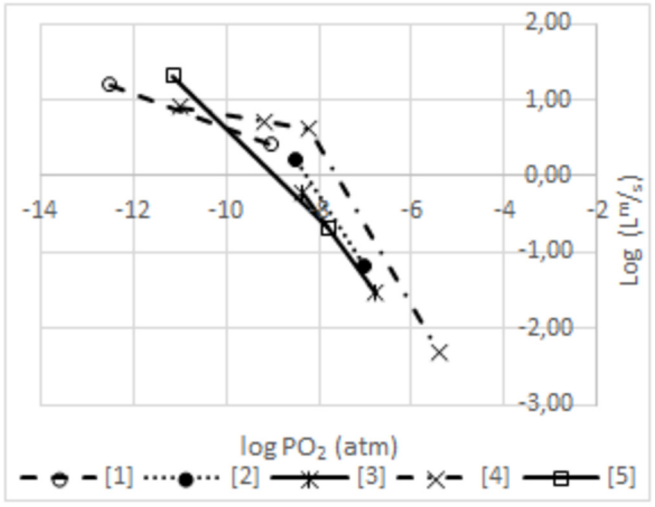

Fig. b. Distribution coefficients of arsenic as a function of pO_2 at 1200 °C. Reproduced from authors [1] Matyas (1975), [2] Rytkönen and Taskinen (1986), [3] Rytkönen and Klarin (1987), [4] Toubarts (1991), [5] Moon et al. (1997) ([1], [2], [4] reproduced from Toubarts (1991); [3] and [5] from original works).

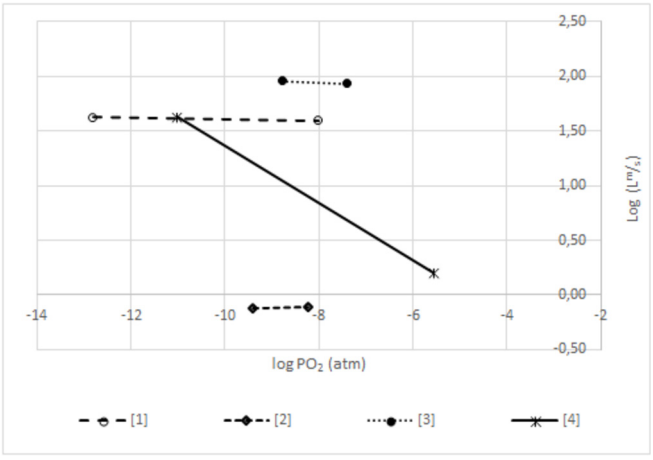

Fig. d. Distribution coefficients for bismuth at 1200 °C. Reproduced from figure of Toubarts (1991) [1] Matyas (1975) [2] Volodchenko et al. (1983) [3] Rytkönen and Taskinen (1986) [4] Toubarts (1991).

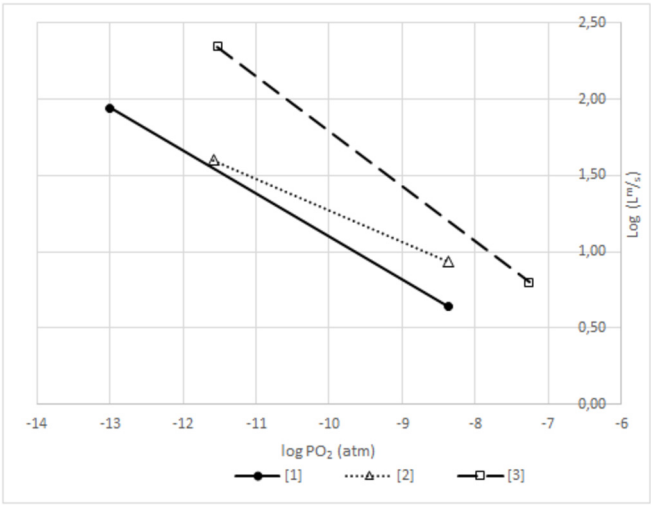

Fig. e. Distribution coefficients for copper between lead and slag from [1] Matyas (1975) with alumina crucible, 1200 °C, [2] Matyas (1975) with zirconia crucible 1200 °C [3] Moon et al. (1997) at 1150 °C.

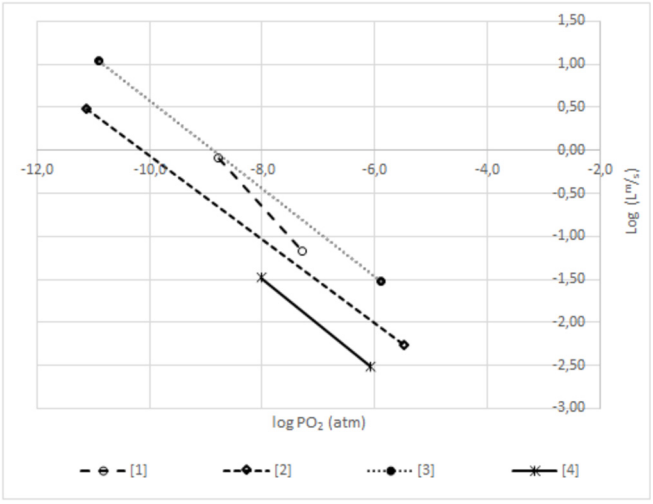

Fig. f. Distribution coefficients for tin [1] Rytkönen and Taskinen (1986) results at 1200 °C. Toubarts (1991) at [2] 1200 °C, [3] 1300 °C, [4] 1150 °C.

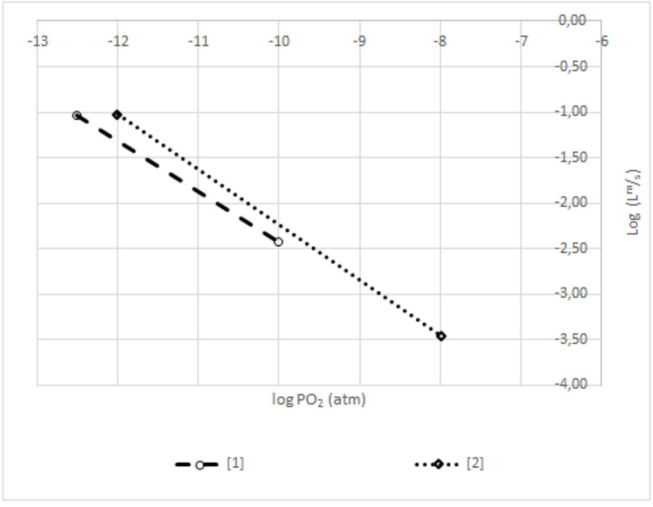

Fig. g. Distribution coefficients for germanium at 1200 °C, recreated from Henao et al. (2010). Ge: Comparison of $L_{Ge}^{s/m}$ for experimental results from [1] Yan and Swinbourne (2003) and [2] Henao et al. (2010).

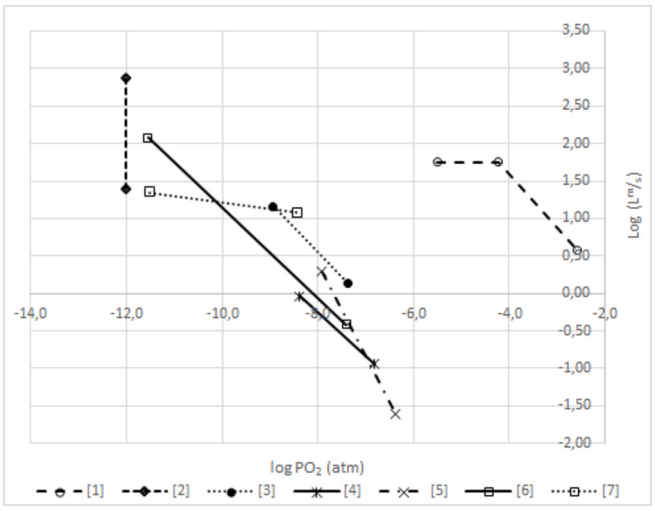

Fig. h. Distribution coefficients for antimony as reported in the range of 1150–1250 °C. [1] Volodchenko et al. (1983), [2] Johnson (1983), [3] Rytkönen and Taskinen (1986), [4] Rytkönen and Klarin (1987), [5] Toubarts (1991), [6] Moon et al. (1997) [7] Matyas (1975) (Matyas Recreated from figure from Rytkönen and Taskinen (1986)).

References

Aldrich, C., Van Deventer, J.S.J., Reuter, M.A., 1994. The application of neural nets in the metallurgical industry. Miner. Eng. 7 (5), 793–809.

Amini, S.H., Remmerswaal, J.A.M., Castro, M.B., Reuter, M.A., 2007. Quantifying the quality loss and resource efficiency of recycling by means of exergy analysis. J. Clean. Prod. 15 (10), 907–913.

Anindya, A., 2012. Minor Elements Distribution during the Smelting of WEEE with Copper Scrap. RMIT University, Melbourne, Australia.

Anindya, A., et al., 2013. Distribution of elements between copper and FeOx–CaO–SiO2 slags during pyrometallurgical processing of WEEE: Part 1–Tin. Miner. Process. Extract. Metall. 122 (3), 165–173.

Anindya, A., et al., 2014. Distribution of elements between copper and FeOx–CaO–SiO2 slags during pyroprocessing of WEEE: Part 2–indium. Miner. Process. Extract. Metall. 123 (1), 43–52.

Antrekowitsch, H., Potesser, M., Spruzina, W., Prior, F., 2006. Metallurgical recycling of electronic scrap. In: EPD Congress, San Antonio, TX, USA, pp. 899–908.

Asaki, Z., Taniguchi, T., Hayashi, M., 2001. Kinetics of the reactions in the smelting furnace of the Mitsubishi process. JOM (J. Occup. Med.) 53 (5), 25–27.

Avarmaa, K., O'Brien, H., Johto, H., Taskinen, P., 2015. Equilibrium distribution of precious metals between slag and copper matte at 1250 -1350°C. J. Sustain. Metall. 1 (3), 216–228.

Avarmaa, K., Johto, H., Taskinen, P., 2016. Distribution of precious metals (Ag, Au, Pd, Pt and Rh) between copper matte and iron silicate slag. Metall. Mater. Trans. B 47 (1), 244–255.

Battle, T.P., Hager, J.P., 1990. Viscosities and activities in lead-smelting slags. Metall. Trans. B 21 (3), 501–510.

Brocken, N.M.P., Olivetti, E.A., Cullen, J.M., Potting, J., Lifset, R., 2017. Taking the circularity to the next level A special issue on the circular economy. J. Ind. Ecol. 21 (3), 476–482.

Cockcroft, S., Richards, G., Brimacombe, J., 1988. Mathematical model of lead behaviour in the zinc slag fuming process. Can. Metall. Q. 27 (1), 27–40.

Dongbo, L., Zunfeng, S., 2010. Oxygen Bottom Blowing Smelting (SKS) Process-electrothermal Bottom Blowing Molten Reduction for Lead Smelting. China ENFI Engineering Corporation. http://www.enfi.com.cn.

Ellen Macarthur Foundation, 2017. Circular Economy. www.ellenmacarthurfoundation.org (accessed 18.11.2017).

Ellis, T.W., Mirza, A.H., 2010. The refining of secondary lead for use in advanced lead-acid batteries. J. Power Sources 195 (14), 4525–4529.

Elvers, B., Hawkins, S., Russey, W., 1989. Ullmann's Encyclopedia of Industrial Chemistry. Wiley Online Library.

Errington, B., Hawkins, P., Lim, A., 2010. Isasmelt for lead recycling. In: Lead-zinc 2010, TMS. John Wiley & Sons, Hoboken, NJ, USA, pp. 709–720.

EU, 2015. Closing the Loop - an EU Action Plan for the Circular Economy. https://ec.europa.eu/growth/industry/sustainability/circular-economy_en (accessed 18.11.2017).

EU, 2017. Directorate-general for internal market, industry, entrepreneurship and SMEs (european commission. In: Study on the Review of the List of Critical Raw Materials. European Commission, Brussels. Retrieved 27-09-2017 from. https://publications.europa.eu/en/publication-detail/-/publication/08fdab5f-9766-11e7-b92d-01aa75ed71a1/language-en.

FactSage, 2015. Thermfact and GTT Technologies. FactSage 7.1. http://gtt-

technologies.de.
Fairphone, Ballester, M., van Schaik, A., Reuter, M.A., 2017. Fairphone's Report on Recyclability-does Modularity Contribute to Better Recovery of Materials? (accessed 19-10-2017). https://www.fairphone.com/en/2017/02/27/recyclable-fairphone-2/. https://www.fairphone.com/en/2017/08/08/examining-the-environmental-footprint-of-electronics-recycling/.
Frenzel, M., Kullik, J., Reuter, M.A., Gutzmer, J., 2017a. Raw material "criticality"-Sense or nonsense? J. Phys. D Appl. Phys. 50 (12), 123002.
Frenzel, M., Mikolajczak, C., Reuter, M.A., Gutzmer, J., 2017b. Quantifying the relative availability of high-tech by-product metals – the cases of gallium, germanium and indium. Resour. Pol. 52, 327–335.
Fisher, G.T., Bennington, K., 1991. Solubility of Lead and Distribution of Minor Elements between Bullion and Calcium Ferrite Slag at 1,250° C. US Department of the Interior, Bureau of Mines.
GaBi, 2017. Thinkstep Stuttgart. www.thinkstep.com (accessed 18-11-2017).
Georgalli, G., Eksteen, J., Reuter, M.A., 2002. An integrated thermochemical-systems approach to the prediction of matte composition dynamics in an Ausmelt® nickel–copper matte converter. Miner. Eng. 15 (11), 909–917.
Greenpeace, 2017. A Guide to Greener Electronics. http://www.greenpeace.org/usa/wp-content/uploads/2017/10/Guide-to-Greener-Electronics-2017.pdf (accessed 18-11-2017).
Guthrie, R.I.L., 1993. Engineering in Process Metallurgy. Oxford University Press, Oxford.
Henao, H., Hayes, P., Jak, E., 2010. Research on indium and germanium distributions between lead bullion and slag at selected process conditions. In: Lead-zinc 2010, TMS. John Wiley & Sons, Hoboken, NJ, USA, pp. 1145–1160.
Hoang, G., Swinbourne, D., 2007. Indium distribution between FeO–CaO–SiO_2 slags and lead bullion at 1200° C. Miner. Process. Extr. Metall. 116 (2), 133–138.
Hollitt, M., 1984a. Measurement and prediction of PbO activities in industrial lead smelting slags. In: Symposium on Extractive Metallurgy. The Aus.I.M.M Melbourne Branch, pp. 69–78.
Hollitt, M., 1984b. Thermodynamics of the Pb-S-O-SiO_2 System at 1200°C. University of Melbourne.
Huda, N., Naser, J., Brooks, G., Reuter, M.A., Matusewicz, R., 2012a. Computational fluid dynamics (CFD) investigation of submerged combustion behavior in a tuyere blown slag-fuming furnace. Metall. Mater. Trans. B 43 (5), 1054–1068.
Huda, N., Naser, J., Brooks, G., Reuter, M.A., Matusewicz, R.W., 2012b. Computational fluid dynamic modeling of zinc slag fuming process in top-submerged lance smelting furnace. Metall. Mater. Trans. B 43 (1), 39–55.
International-Lead-and-Zinc-Study-Group, 2017. Lead and Zinc Statistics. Retrieved 25-08-2017, from. http://www.ilzsg.org/static/statistics.aspx?from=1.
International-Lead-Association, 2012. Lead Uses-Statistics. Retrieved 25-08-2017, from. www.ila-lead.org/lead-facts/lead-uses–statistics.
Jak, E., Hayes, P.C., Lee, H., 1995. Improved methodologies of the determination of high temperature phase equilibria. Met. Mater. 1 (1), 1–8.
Jak, E., 2012. Integrated experimental and thermodynamic modelling research methodology for metallurgical slags with examples in the copper production field. In: Proceedings of IX International Conference on Molten Slags, Fluxes and Salts. Chinese society for metals, Beijing, China. May 2012.
Jak, E., Hayes, P., 2010. Phase Chemistry of Lead Smelting Slags" Lead-Zinc 2010, TMS. John Wiley & Sons, Hoboken, NJ, USA, pp. 1161–1176.
Johnson, E., 1983. Laboratory Investigations on the Behavior of Accessory Elements in Lead Blast Furnace Smelting. U. S. Dept. of Interior, pp. 1–17.
Kawahara, M., Doi, T., Moringa, K., Yaganase, T., 1979. The behavior of arsenic in slag melts. J. Min. Metall. Inst. Jpn. 95 (1102), 877–882.
Kawai, Y., Shinozaki, N., Mori, K., 1982. Rate of transfer of manganese across metal-slag interface and interfacial phenomena. Can. J. Metall. Mater. Sci. 21 (4), 385–391.
Kinaev, N., Jak, N.E., Hayes, P.C., 2005. Kinetics of reduction of lead smelting slags with solid carbon. Scand. J. Metall. 34 (2), 150–157.
Klemettinen, L., Avarmaa, K., Taskinen, P., 2017. Trace element distributions in black copper smelting. World Metall. Erzmetall 70 (5), 257–264.
Kudo, M., Jak, E., Hayes, P., Yamaguchi, K., Takeda, Y., 2000. Lead solubility in FeOx-CaO-SiO_2 slags at iron saturation. Metall. Mater. Trans. B 31 (1), 15–24.
Kyllo, A.K., Richards, G.G., 1998. Kinetic modeling of minor element behavior in copper converting. Metall. Mater. Trans. B 29 (1), 261–268.
Matsura, Dai, Ueda, Shigeru, Yamaguchi, Katsunori, 2011. Lead Solubility in FeOx-CaO-SiO2-NaO0: 5 and FeOx-CaO-SiO2-CrO1: 5 Slags under Iron Saturation at 1573 K. High Temp. Mater. Process. 30 (4-5), 441–446.
Matyas, A., 1975. Solubility of lead in lead blast furnace slags. In: Foroulis, Z.A., Smeltzer, W.W. (Eds.), Metal–slag–gas Reactions and Processes. The Electrochemical Society, Inc, Princeton, NJ, pp. 999–1011.
Messner, T., Pogatscher, S., Pesl, H.A.J., 2007. Thermodynamic modelling of the behaviour of accompanying elements in secondary copper production. In: Proceedings of EMC, vol. 2007, pp. 1819–1837.
Moon, M.H., Lee, Y., Igataki, K., 1997. PbO activity and impurity dissolution in PbO-FeOx-CaO-SiO_2 slag. In: Proceedings of the 5 Th International Conference on Molten Slags, Fluxes and Salts, pp. 753–759. 97-Jan 5-8, 1997, Sydney, Australia.
Outotec, 2017a. Flash Smelting and TSL Technology. http://www.outotec.com/products/?category=80 (accessed 18-11-2017).
Outotec, 2017b. HSC Chemistry 9 Outotec. http://www.outotec.com/products/digital-solutions/hsc-chemistry (accessed 18-11-2017).
Perez-Tello, M., Prieto-Sanchez, M.R., Rodriguez-Hoyos, O., Sanchez-Corrales, V.M., 2004. A kinetic model for the oxidation of selenium and tellurium in an industrial Kaldo Furnace. JOM (J. Occup. Med.) 56 (12), 52–55.
Pomfret, R., Grieveson, P., 1983. The kinetics of slag-metal reactions. Can. Metall. Q. 22 (3), 287–299.
Reuter, M.A., Van der Walt, T., Van Deventer, J.S.J., 1992. Modeling of metal-slag equilibrium processes using neural nets. Metall. Trans. B 23, 643–650.
Reuter, M.A., Matusewicz, R., Van Schaik, A., 2015a. Lead, zinc and their minor elements: enablers of a circular economy. World Metall. Erzmetall 68 (3), 132–146.
Reuter, M.A., Van Schaik, A., Gediga, J., 2015b. Simulation-based design for resource efficiency of metal production and recycling systems: cases-copper production and recycling, e-waste (LED lamps) and nickel pig iron. Int. J. Life Cycle Assess. 20 (5), 671–693.
Reuter, M.A., 2016. Digitalizing the circular economy-circular economy engineering defined by the metallurgical internet of things-, 2016 TMS EPD distinguished lecture, USA. Metall. Trans. B 47 (6), 3194–3220.
Richards, G.G., Brimacombe, J., Toop, G., 1985. Kinetics of the zinc slag-Fuming process: Part I. industrial measurements. Metall. Mater. Trans. B 16 (3), 513–527.
Rönnlund, I., Reuter, M.A., Horn, S., Aho, J., Päällysaho, M., Ylimäki, L., Pursula, T., 2016. Implementation of sustainability indicator framework in the metallurgical industry: Part 2-A case study from the copper industry. Int. J. Life Cycle Assess. 21 (12), 1719–1748.
Rytkönen, T., Klarin, A., 1987. Distribution equilibria of impurities between lead and calcium ferrite slags. Scand. J. Metall. 16 (5), 210–213.
Rytkönen, T., Taskinen, A., 1986. Distribution of impurities between lead and lead silicate slags. Scand. J. Metall. 15 (1), 25–29.
Shevchenko, M., Jak, E., 2017. Experimental liquidus studies of the Pb-Fe-Si-O system in equilibrium with metallic Pb. Metall. Mater. Trans. B 1–22.
Schlesinger, M.E., 1986. PbO solubility in lead-blast furnace slags. Metall. Mater. Trans. 17 (4), 817.
Schriner, D., Taylor, P., Grogan, J., 2016. A review of slag chemistry in lead recycling. In: Advances in Molten Slags, Fluxes and Salts: Proceedings of the 10th International Conference on Molten Slags, Fluxes and Salts, 2016. Springer, Cham, pp. 879–888.
Shuva, M.A.H., Rhamdhani, M.A., Brooks, G., Masood, S., Reuter, M.A., 2016a. Thermodynamics behaviour of germanium during equilibrium reactions between FeOx-CaO-SiO_2-MgO slag and molten copper. Metall. Trans. B 47 (5), 2889–2903.
Shuva, M.A.H., Rhamdhani, M.A., Brooks, G., Masood, S., Reuter, M.A., 2016b. Thermodynamics data of valuable elements relevant to e-waste processing through primary and secondary copper production: a review. J. Clean. Prod. 131, 795–809.
Shuva, M.A.H., Rhamdhani, M.A., Brooks, G., Masood, S., Reuter, M.A., 2017. Thermodynamics behaviour of palladium and tantalum during equilibrium reactions between FeO_x-CaO-SiO_2-MgO slag and molten copper. Metall. Trans. B 48 (1), 317–327.
Siegmund, A.J., 2000. Primary lead production-a survey of existing smelters and refineries. In: Dutrizac, J.E., Gonzalez, J.A., Henke, D.M., James, S.E., Siegmund, A.H.J. (Eds.), Lead-zinc 2000. TMS, Warrendale, pp. 53–116.
Sohn, H.S., Fukunaka, Y., Oishi, T., Sohn, H.Y., Asaki, Z., 2004. Kinetics of As, Sb, Bi and Pb volatilization from industrial copper matte during Ar+ O2 bubbling. Metall. Mater. Trans. B 35 (4), 651–661.
Sutherland, C.A., Milner, E.F., Kerby, R.C., Teindl, H., Melin, A., Bolt, H.M., 2013. Lead" Ullmann's Encyclopedia of Industrial Chemistry. Wiley Online Library.
Swinbourne, D.R., Kho, T.S., 2012. Computational thermodynamics modeling of minor element distributions during copper flash converting. Metall. Mater. Trans. B 43B, 823–829.
Takeda, Y., Nakazawa, S., Yazawa, A., 1980. Thermodynamics of calcium ferrite slags at 1200 and 1300 °C. Can. Metall. Q. 19 (3), 297–305.
Takeda, Y., Ishiwata, S., Yazawa, A., 1983. Distribution equilibria of minor elements between liquid copper and calcium ferrite slag. Trans. Jpn. Inst. Metals 24 (7), 518–528.
Taskinen, A., Toivonen, L., Talonen, T., 1984. Thermodynamics of slags in direct lead smelting. In: Fine, H.A., Gaskell, D.R. (Eds.), Second International Symposium on Metallurgical Slags and Fluxes. TMS-AIME, Warrendate, PA, pp. 741–756.
Timucin, M., 1980. Thermodynamic properties of liquid copper-lead alloys. Metall. Mater. Trans. B 11 (3), 503–510.
Toubarts, 1991. Blei-Schlacken-Verteilungsgleichgewichte unter oxidierenden und reduzierenden Bedingungen. Diplom-Ingenieur thesis. Rheinisch-Westfälischen Technischen Hochschule Aachen.
Trinks, W., Mawhinney, M., Shannon, R., Reed, R., Garvey, J., 2004. Industrial Furnaces. Wiley-Intersciences.
UNEP, 2013. A Report of the Working Group on the Global Metal Flows to the International Resource Panel. In: Reuter, M.A., Hudson, C., Van Schaik, A., Heiskanen, K., Meskers, C., Hagelüken, C. (Eds.), Metal Recycling: Opportunities, Limits, Infrastructure. Retrieved: 11-09-2017, from. http://www.resourcepanel.org/reports/metal-recycling.
Van Schaik, A., Reuter, M.A., 2014. Chapter 22: material-centric (Aluminium and Copper) and product-centric (Cars, WEEE, TV, lamps, batteries, catalysts) recycling and DfR rules. In: Worrell, E., Reuter, M.A. (Eds.), Handbook of

Recycling. Elsevier, pp. 307–378.
Verhoef, E., Dijkema, G., Reuter, M.A., 2004. Process knowledge, system dynamics and metal ecology. J. Ind. Ecol. 8 (1–2), 23–43.
Volodchenko, S., Vaskevich, A., Sorokin, M., 1983. A study into the behavior of accompanying elements in the equilibrium lead–slag–gas phase. Sov. J. Non Ferrous Met. 24 (10), 28–31.
Yan, S., Swinbourne, D., 2003. Distribution of germanium under lead smelting conditions. Miner. Process. Extr. Metall. (IMM Trans. Sect. C) 112 (2), 75–80.
Yazawa, A., Takeda, Y., 1982. Equilibrium relations between liquid copper and calcium ferrite slag. Trans. Jpn. Inst. Metals 23 (6), 328–333.
Yazawa, A., Takeda, Y., Waseda, Y., 1981. Thermodynamic properties and structure of ferrite slags and their process implications. Can. Metall. Q. 20 (2), 129, 13.